

Marple Simulations of the Plasma MFC Scheme¹

V.A. Gasilov, A.S. Chuvatin,* S.V. D'yachenko, O.G. Olkhovskaya, E.L. Kartasheva,
A.S. Boldarev, V.I. Oreshkin,**

Institute for Mathematical Modeling, Russian Academy of Sciences, Miusskaya Sq. 4a, Moscow, 125047, Russian Federation, Tel (7-495) 250 79 39, Fax (7-495) 972 07 23, E-mail Gasilov@yandex.ru

**Laboratoire de Physique et Technologie des Plasmas, Ecole Polytechnique, Palaiseau, 91128, France*

***Institute of High Current Electronics, Russian Academy of Sciences, 2/3 Akademicheskoy Avenue, Tomsk, 634055, Russian Federation*

Abstract – Numerical radiative magnetohydrodynamics is an essential part of the modern high-energy-density physics and pulse-power research. In this work we report numerical studies of a power multiplication scheme based on compression of magnetic flux by plasmas shells suggested in [1, 2]. Confinement of the magnetic flux by a plasma having self-adjustable thickness of the order of the skin depth is not evident *a priori* and efficiency of the considered scheme may depend on numerous physical parameters such as plasma thermodynamic properties or radiative losses. The reported results are obtained with the help of new Marple code [3] incorporating the most part of physical properties that may lead to the flux losses for the current amplitudes ranging from one to several MA with the rise-time of 10^2 - 10^3 ns. By comparing the numerical results with simple estimates, we demonstrate that operation of the studied scheme indeed results in current pulse sharpening and power multiplication. Influence of the amplitude of the initially seeded magnetic field on the scheme efficiency is discussed.

1. Introduction

Magnetic Flux Compression (MFC) represents one of the modern promising schemes realizing magnetic energy storage with further energy compression in space and time. In particular, this scheme implies that an accelerated conductor can compress the flux of initially seeded azimuthal magnetic field. As it was first suggested in [1, 2], the accelerating force can be the Lorentz force of current created by a pulse-power generator. The generator produces the primary magnetic field accelerating a plasma shell (plasma MFC) which is supposed to compress and amplify the inner (secondary) magnetic field associated with the load current. This technique implies initiation of a hollow

plasma cylinder from gas puffs, dielectric films or conducting foils. Therefore, in difference with the previous extensive MFC application at magneto-explosive generators the maximum shell velocity is determined by the Alfvén velocity rather than by thermal velocity of explosion products. This opens possibilities for shortening of the load current pulse rise-time to ~ 100 ns and below.

Numerical, rather than experimental evaluation of the scheme feasibility becomes of particular importance when the experiments require energies of many megajoules. Numerical modeling could thus reveal physical limitations on the scheme operation efficiency and could play a determining role in engineering development of future thermonuclear facilities.

Despite limited experimental information available for the plasma MFC scheme, its theoretical efficiency was already investigated analytically and in simplified one-dimensional (1D) numerical modeling [4, 5]. One of the identified theoretical limitations on the scheme efficiency is related to diffusion of the compressed magnetic flux into the plasma of accelerated shell. In this case, a part of the flux remains frozen in the plasma during the short time of the load current increase and, therefore, can penetrate the load only with the plasma. In this work, we continue the study of this limitation in two-dimensional (2D) geometry close to the experimental one. The plasma MFC scheme is studied below in cylindrical geometry with Eulerian code Marple based on unstructured grid computation technology. The incorporated physics includes the resistive two-temperature Braginskii model with radiative term calculated through solution of the radiation transport equation in Schwarzschild-Schuster approximation [3]. The scheme is considered for two types of pulse-power loads used either in isentropic compression experiment [6] or for creation of plasma radiation sources [1, 2].

¹ The work was supported by Centre d'Etudes de Gramat (France) under the contract n° 03-097/HA and by International Science & Technology Center under the project ISTC-2830. The authors are grateful to the Russian Science Support Foundation for support of the work done by V.I. Oreshkin.

2. Plasma MFC application in isentropic compression experiments

The geometry of Fig. 1 corresponds to compression of the magnetic flux in a vacuum load region in order to generate high magnetic pressures in experiments on isentropic compression of materials and in study of the equations of state [6]. The primary generator is connected on the right boundary of the simulation region and it represents an ideal generator of the current which rises as sine function up to the maximum value $I_{1\max} = 3$ MA during the quarter-period $t_1 = 1$ μ s. The secondary current with the amplitude I_2 is injected at the initial moment of time between the plasma shell and the stator. In 2D numerical simulation, we were primarily interested by limitation on the plasma MFC scheme efficiency due to magnetic flux losses in the plasma. Therefore, macro-instabilities of the shell plasma were not initiated in our modeling.

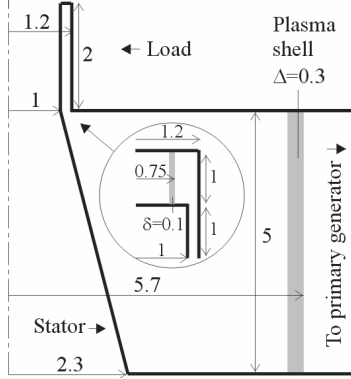


Fig. 1. Simulation region for the plasma MFC problem with constant-inductance load described in Section 2. The insert shows the second plasma shell in the load used in simulations described in Section 3. All sizes are in centimeters

Consider first the geometry of Fig. 1 with an infinitely thin, perfectly conducting shell of the mass M accelerated and decelerated by the difference of magnetic pressures in the primary and secondary circuits. The load represents a constant inductance with the value $L_d \sim 0.73$ nH calculated from the electrodes geometry of Fig. 1. Conservation of the secondary magnetic flux implies $(L + L_d)I_2(t) = \text{const}$, where L is the varying inductance between the liner and the stator. The equations describing evolution of the system are:

$$\frac{M}{h} \frac{d^2 R}{dt^2} = -\frac{1}{c^2 R(t)} (I_1^2 - I_2^2) \quad (1)$$

$$\left[L_d + 2h \ln(R(t)/r_s) \right] I_2 = \text{const}$$

where $R(t)$ and $h = 5$ cm are the radius and the height of the liner, r_s is the stator radius. The constant in the second expression is defined by the initial liner radius and by the initial current in the secondary circuit.

When the liner impacts the stator, it is further considered as motionless.

Let us first define $I_2 = 300$ kA as the initial secondary current value and consider the mass of the liner - magnetic compressor $M = 2.5$ mg. The time-dependencies of the secondary current $I_2(t)$ were found from the system (1) and they were further compared to 2D Marple modeling. For this comparison, the magnetic field and plasma density were measured by load probes situated at the external load electrode at the radius $r = 1.2$ cm and at different heights: from $z = 5$ cm (entry to the load region) up to $z = 7$ cm (the upper right corner in Fig. 1). Comparison of the probe signals at different positions allows evaluation of axial inhomogeneity of the calculated values.

Upper curves in Fig. 2 illustrate comparison of the 0D current in the secondary with the current measured by the probes in 2D simulations for the above-described MFC parameters.

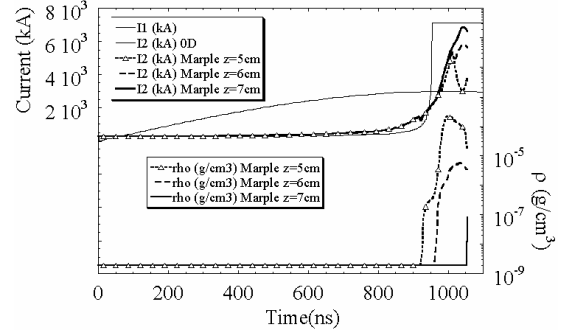


Fig. 2. Comparison of 0D estimates of the secondary current with the values obtained in 2D Marple simulations (upper curves). Initial secondary current value is $I_2 = 300$ kA. Lower curves correspond to the plasma density measured at the same points as the values of I_2

As it can be seen from this figure, the Marple result for I_2 and the corresponding result from the 0D estimate reveal substantial difference. This difference appears due to the finite thickness of the plasma-compressor, which is not taken into account in 0D estimate of Eq. (1). Indeed, as it was already mentioned above, the shell thickness is auto-established during diffusion of both the primary and the secondary magnetic fields into the plasma [5]. As a result, a part of the secondary flux is compressed with the plasma slower than by an infinitely thin 0D shell, and the final compression time is defined by the shell thickness and velocity.

The secondary current probe signals in 2D also differ at different heights ($z = 5, 6,$ and 7 cm). Explanation of this result can be found in the plasma density measurements at the same space points (Fig. 2). The magnetic field seems to be convected into the load region being magnetized into the plasma. This hypothesis is confirmed by the 2D plasma density map in Fig. 4 at the moment close to the maximum flux

compression. The frozen part of the secondary flux may penetrate the load only with the liner plasma and, as it can be seen in Fig. 3 for $z = 5$ cm, the condition $B/\rho = \text{const}$ is approximately satisfied. Plasma inertia further makes the load current increase to be substantially slower than that defined by the ideal electromagnetic process of Eq. (1). Besides, this effect may lead to inhomogeneity of the magnetic field along the studied material in isentropic compression experiments [6]. In order to avoid this undesirable effect, one could suggest to increase the initial value of the secondary current.

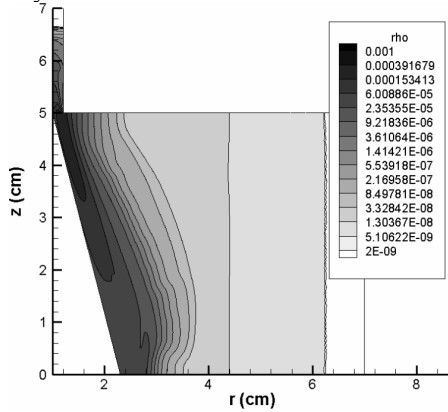


Fig. 3. Plasma density map ρ in g/cm^3 for $t = 1 \mu\text{s}$ when the liner plasma penetrates into the load region

Fig. 4 shows results of the 0D estimate upon Eq. (1) together with the 2D Marple modeling for a modified problem statement, when the initial secondary current was increased to the value $I_2 = 1$ MA and the plasma liner mass was chosen to be $M = 1.55$ mg.

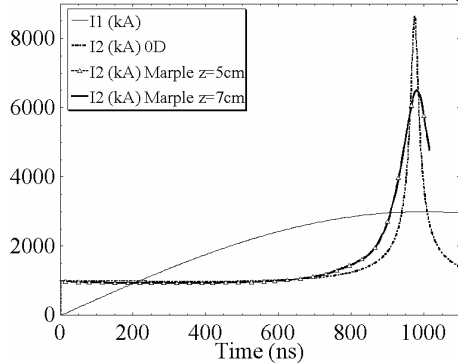


Fig. 4. Comparison of the 0D estimate for secondary current, Eq. (1), with the value obtained in Marple 2D simulation. Initial secondary current has the value of $I_2 = 1$ MA. The $I_2(t)$ curves at different heights now coincide

As it can be seen in Fig. 4, a good agreement is now observed between 0D and 2D. One may assume that this better agreement (if compared to Fig. 3) at higher initial secondary current is achieved due to the fact that the main liner mass is now decelerated and even rebounds from the stator. This partially attenuates the effect of finite shell thickness and of the mag-

netic flux losses in the plasma. Besides, the magnetic field pressure is now homogeneous with excellent accuracy along the inductive load. Indeed, the shin shell in 0D estimate (Fig. 4) does not reach the stator radius $r_s = 1$ cm and rather starts to expand in opposite direction. The same effect, which is due change of the sign of magnetic pressures in Eq. (1) is reproduced in 2D modeling, Fig. 5.

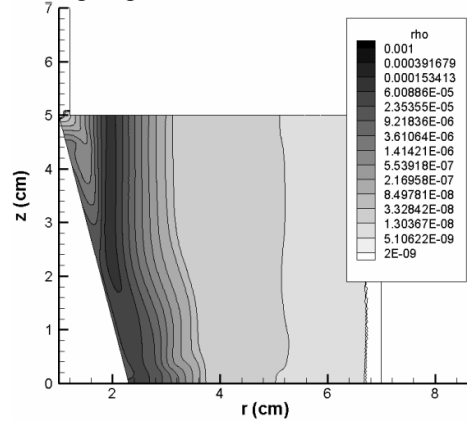


Fig. 5. Plasma density map in g/cm^3 at $t = 985$ ns, corresponding to the maximum magnetic flux compression and beginning of the plasma shell bouncing. The initial secondary current value is increased from 300 kA to 1 MA

As shows Fig. 5, the increase of the load magnetic energy is now realized purely in vacuum, i.e. without penetration of the liner plasma into the load region. It can signify that in this Marple modeling we found a configuration, which is closer to the optimum in the MFC isentropic compression problem. Besides, the plasma bouncing signifies better realization of the liner kinetic energy. This would partially compensate higher energy spent on creation of the seeded magnetic flux in the secondary. Indeed, despite the higher magnetic pressure in the secondary, the peak I_2 current value is practically the same (6-7 MA) for the initial $I_2 = 1$ MA and in the previous case of initial $I_2 = 300$ kA (compare the results of Figs. 2 and 4).

3. Numerical modeling of the plasma MFC scheme operating with a liner load

Let us consider now a more complex geometry, in which the MFC scheme is used for formation of a pulsed current in a pinch-type load [1, 2]. The problem geometry is shown in Fig. 1, where the load is represented now by a plasma liner. In this configuration, the usage of magnetic compressor theoretically allows to obtain smaller load current rise-times if compared to the direct generator-to-load connection.

In difference with the simulations described above, the primary was represented by sine-shaped current with the amplitude $I_{1max} = 20$ MA and the quarter-period of $t_1 = 200$ ns. To avoid the current prepulse in the plasma liner load, the secondary current I_2 was

now injected at $t = 100$ ns and, starting from this moment, I_2 rises as a sine function to the maximum value I_{2max} during $\Delta t = 50$ ns.

Fig. 6 illustrates the 2D Marple result for the secondary current amplitude equal to $I_{2max} = 2$ MA, for the liner-compressor mass equal to $M = 5$ mg and for the load liner mass equal to $M_d = 0.5$ mg. The probe positions for the magnetic field and plasma density measurements are the same as in the result of Fig. 2.

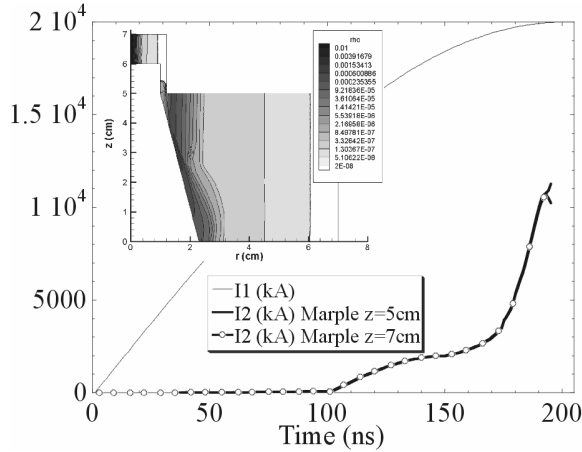


Fig. 6. Secondary current I_2 measured in 2D simulation at two axial positions in the load, $r = 1.2$ cm, $z = 5$ cm and $z = 7$ cm (the results coincide). Secondary current amplitude is $I_{2max} = 2$ MA. The insert is the plasma density map at $t = 195$ ns, close to the maximum load current. The load kinetic energy is 120 kJ

Following our discussion of the simulation with constant load inductance, Fig. 6 shows that the secondary current amplitude is chosen to be sufficiently high to avoid penetration of the compressor plasma into the load region. At the same time, the chosen parameters did not allow increase of the load current over the generator current. However, the current rise-time, which is directly due to the flux compression was less than 50 ns.

Let us define relationships describing the 0D dynamics of compression of both plasma shells presented in Fig. 1 (both shells are considered as infinitely thin). Eq. (1) still holds, but the load inductance is now variable and determined by the equation of motion.

$$L_d(t) = L_{d0} + 2h_d \ln(R_d/r_d(t)) \quad (2)$$

$$\frac{M_d}{h_d} \frac{d^2 r_d}{dt^2} = -\frac{I_2^2}{c^2 r_d}$$

where h_d , $r_d(t)$, M_d correspond to the z -pinch height, initial and current radius, and the mass. $R_d = 1.2$ cm is the current return radius. Assume that the z -pinch shell is 10-fold compressed and then its motion is stopped. Eqs. (1, 2) suggest optimization of the load

geometry for the plasma MFC scheme. Consider the load liner of 0.5 cm height, having the mass of 7 mg, with the initial radius of 0.5 cm and with the current return having the radius of 0.7 cm in Fig. 1. Fig. 7 shows solution of Eqs. (1, 2) for the same primary and secondary generators as in Fig. 6.

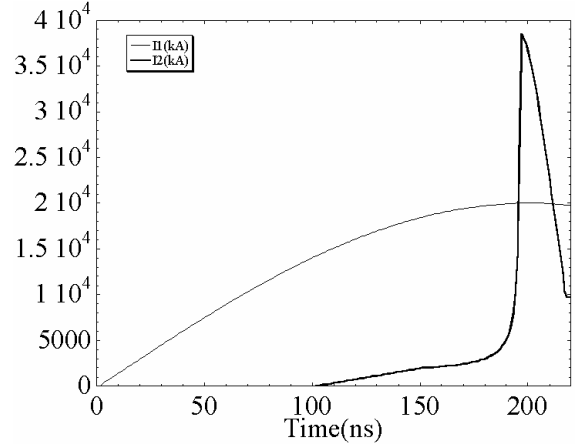


Fig. 7. A 0D estimate from Eqs. (1, 2) obtained for decreased load size with respect to Fig. 1 and for the pinch mass of $M_d = 7$ mg. The load kinetic energy is 490 kJ

As it can be seen, the decrease of the load dimensions in the plasma MFC scheme may allow a 3-fold decrease of the load walls surface and a considerable increase of the load current amplitude and of the pinch kinetic energy. Indeed, we efficiently decreased the maximum load inductance L_d and, as a consequence, we increased the maximum achievable secondary current ($I_2 \sim 1/L_d$, see Eq. (1)). We also increased the pinch mass, allowing higher secondary current in the load before the pinch shell is considerably displaced. This resulted in higher kinetic energy capable to be radiated onto a lower wall surface in the load that opens perspectives for further plasma MFC optimization for high energy density physics experiments.

References

- [1] J.F.Leon, R.B.Spielman, et al, in *Proc. 12th IEEE Int. Pulsed Power Conf.*, 1999, p. 275.
- [2] P.L'Eplattenier, M.Bavay et al, in *Proc. 13th IEEE Int. Pulsed Power Conf.*, 2001, p. 665.
- [3] V.A.Gasilov, A.S.Chuvatin, et al, *Mathematical Modeling* **15**, 107 (2003).
- [4] A.S.Chuvatin, L.I.Rudakov, and A.L.Velikovich, *Bull. Am. Phys. Soc.* **46**, 316 (2001).
- [5] L.I.Rudakov, A.S.Chuvatin, et al, *Phys. Plasmas* **10**, 4435(2003).
- [6] R.Cauble, D.B.Reisman, et al, *J. Phys.: Condens. Matter* **14**, 10821 (2002).